



## Performance Optimization for Mechanical Properties and Corrosion Resistance of Mg-Al Rolled Alloy with Zn Nano-Coating

F. Q. Mohammed<sup>1</sup> • A. S. Hasan<sup>2</sup> and M. A. A. Musafir<sup>3\*</sup>

<sup>1</sup>Production Engineering and Metallurgy Department,  
University of Technology-Iraq, Baghdad, Iraq

<sup>2,3</sup>Polymer Engineering and Petrochemical Industries Department,  
College of Materials Engineering, University of Babylon, Babylon, Iraq

Received: 21 11 2024; Accepted: 01 26 2025

Available: 28 02 2026

**Abstract:** Magnesium alloy castings and wrought products have many applications in the transportation industry due to their high strength-to-weight ratio. Unfortunately, the highly reactive magnesium materials are susceptible to natural deterioration; thus, the mechanical properties of magnesium alloys must be enhanced to meet the requirements of many applications, as must their chemical behavior. To solve this problem, the Mg-Al alloy was hardened mechanically by cold and warm rolling before Zn nanocoating. The rolled alloy showed a different morphology where the microstructure has deformed and refined with the fragmentation in the  $\beta$ -phase from 50 $\mu\text{m}$  for the as-received samples to about 20 $\mu\text{m}$ . A Zn coating layer with a thickness of approximately 23 micrometers was successfully achieved after a sputtering interval of 20 minutes, due to a longer deposition time for the zinc coating layer. The hardness has improved as deformation increased, as evidenced by a reduction in the thickness of the rolled samples. X-ray diffraction patterns show that twinning has been significantly activated in the rolled alloy compared with the as-received alloy. Geometric designs of the alloy have improved the mechanical properties and corrosion resistance of Mg alloys.

**Keywords:** magnesium alloy, cooled rolling, sputtering, nano-coating, Zn coating.

\*Corresponding author.

E-mail address: [mat.mustafa.a@uobabylon.edu.iq](mailto:mat.mustafa.a@uobabylon.edu.iq) (M.A.A. Musafir).

Peer Review under the responsibility of Universidad Nacional Autónoma de México.

## 1. Introduction

Designers have widely used magnesium alloys due to their relatively low density, which is only two-thirds of the density of aluminum alloys when used for the same application. Thus, it could be an innovative technology if used in the manufacture of lightweight structures. (Monteiro et al., 2012; Musfirah & Jaharah, 2012) However, the low-weight material's mechanical properties and its corrosion resistance must be optimized to be suitable for use in applications requiring high mechanical strength and chemical stability. (Göken et al., 2003) This was the driving force for the dramatic improvements that have been demonstrated for new lightweight alloys, which led to greater interest in magnesium alloys for aerospace and specialty applications. (Li et al., 2014; Lu et al., 2011; Ang, 2021) Recently, many approaches have been adopted to improve these properties via various coating physical and chemical techniques using different coating materials such as titanium, chromium, and zinc. (Lu et al., 2008; Hassan et al., 2024a) These coatings have improved the surface quality of the magnesium alloy against wear and corrosion conditions. (Wang et al., 2003; Nikulin et al., 2010; Al-Maamori et al., 2024) In particular, zinc coatings have been commonly used as protective coatings on magnesium alloys either by physical vapor deposition (PVD) or chemical vapor deposition (CVD). Zinc coatings act as anti-corrosion barriers against corrosive media when magnesium alloy is exposed to a wet environment. (Lu et al., 2019) Sputtering is a PVD technique commonly used to deposit coatings and thin films with excellent adhesion to substrates. (Friedlmeier et al., 1999; Hasan et al., 2020; Ata et al., 2022; Kadem et al., 2020) The advantages of sputtering over other PVD or CVD techniques are the low-temperature deposition so no grain growth occurs, no need for a higher vacuum degree for deposition, and higher adhesion of the fine-grained coating. (Friedlmeier et al., 1999; Akraa et al., 2020; Kadhim et al., 2021) Thus, the sputtering would achieve improved functional properties of a coating that may lead to extending the life expectancy of coated parts. (Akraa et al., 2020; Kadhim et al., 2021; Sharma et al., 2021) In this study, the as-received Mg-8.5%Al alloy was subjected to two modification procedures to improve its bulk mechanical properties. This was achieved through cold and warm rolling (Hardening). The second protocol was performed to increase the corrosion resistance of the Mg-rolled alloy by depositing a thin nano-zinc surface layer via sputtering. The microstructure and Mechanical properties were investigated to evaluate the efficiency of this process by

the geometric optimization design calculations using Gaussian 06 View software and Gaussian 09 software package, by time-dependent density functional theory (TDDFT) with B3LYP function and basis set 6-31G (d,p), respectively.

## 2. Materials and methods

A commercial magnesium alloy bar composed of Mg-Al-Zn was employed in this study. The chemical composition of the alloy, as determined by energy-dispersive spectroscopy, is shown in Table 1. The as-received alloy bar was cut into slices using a wire-cut machine with dimensions of (50×5×3) mm<sup>3</sup>. To avoid cracking in the slice sample, the rolling cylinders were heated to 100 °C for 10 minutes, then each slice sample was subjected to rolling at 100 °C for a different number of passes. The sputtering coating was achieved using the VTC-16-DC sputtering equipment, which consists of a desktop Coater via Plasma Sputtering with a height-adjustable sample holder equipped with a three-target head, suitable for metal coatings only. For the sputtering process parameters used for this coating process, a flow rate of 1.5 cm<sup>3</sup>/min for argon gas, a vacuum pressure of 10-1 Torr, and a current of 20 mA were used, with a deposition time of 15 minutes.

The as-received, rolled, and coated specimens were analyzed using optical microscopy, scanning electron microscopy, and energy-dispersive spectroscopy. The grain size measurements and other microstructural observations were analyzed. The diffraction patterns of the samples were analyzed using X-ray diffraction, and then the crystalline size and dislocation density were calculated for all samples. Performance optimization geometric design calculations were performed using Gaussian 06 View and Gaussian 09 software packages to assess the physical-chemical compatibility of the elements using time-dependent density functional theory (TDDFT) with the B3LYP functional and the 6-31G (d,p) basis set, respectively.

## 3. Results And Discussion

The as-received alloy and the rolled one are shown in Fig. 1, as seen by the optical and scanning electron microscopies. The as-received microstructure is composed of two main phases: the  $\alpha$ -Mg matrix phase which appears in a dark appearance and the coarse lamellar  $\beta$ -phase (Mg<sub>17</sub>Al<sub>12</sub>) which appears in a white appearance as shown in Fig. 1 (a, b). The average grain size was about 50  $\mu$ m and the grain boundaries were covered by lamellar  $\beta$ -phase.

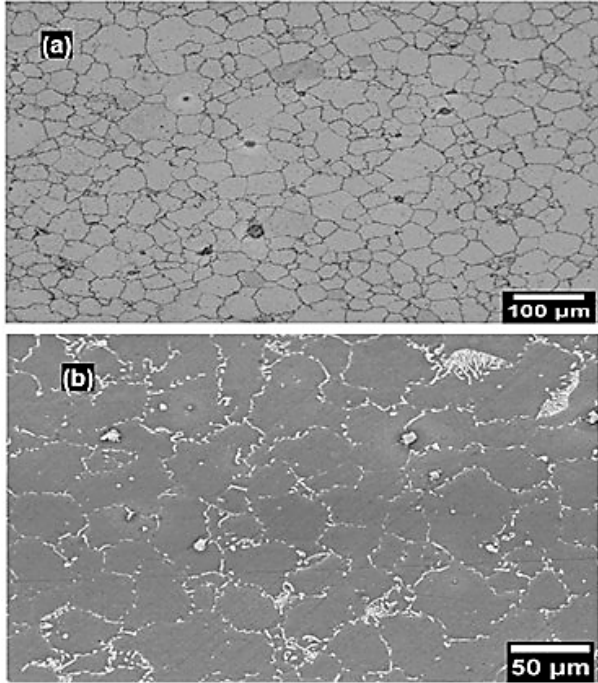


Figure 1. As-received samples of magnesium alloy as seen by optical microscopy (top) and electron scanning microscopy (bottom).

Table 1. Elemental compositions in the as-received.

Element	Mg	Al	Zn
wt.%	Bal.	8.5	0.6

The rolled alloy showed a different morphology where the microstructure has deformed and refined with the fragmentation in the  $\beta$ -phase as shown in Fig. 2 (a-c). The average grain size was about 10  $\mu\text{m}$  and the particle size of the  $\beta$ -phase was about 1  $\mu\text{m}$ . The microstructural grain refinement can be attributed to the imposed strain during the rolling process at room temperature. The refinement is assumed to occur by subdivision of elongated grains via accumulated dislocations and twins. The grain morphology was altered from the coarse-equiaxed to elongated ones by the virtue of rolling-imposed strain as seen in Fig. 2 (c). Further rolling has resulted in intersections between these elongated grains, followed by subdivision of each other into finer grains (Mohammed et al., 2021).

The surface morphology for the Zn coating on the Mg alloy rolled surface is shown in Figure 3. From our previous work, the Zn sputtering deposition at short deposition

time (below 15 min.) can result in a non-homogeneous amorphous surface that will be characterized by a longitudinal micro void that is formed in the coating's surface due to the short deposition time, leading to a decrease in the amount of coating material deposited. In fig.3 the morphology of coated rolled Mg alloy show a dense microstructure with uniform coating and no visible micro voids with a nano-crystalline fiber structure that can be detected in this samples.

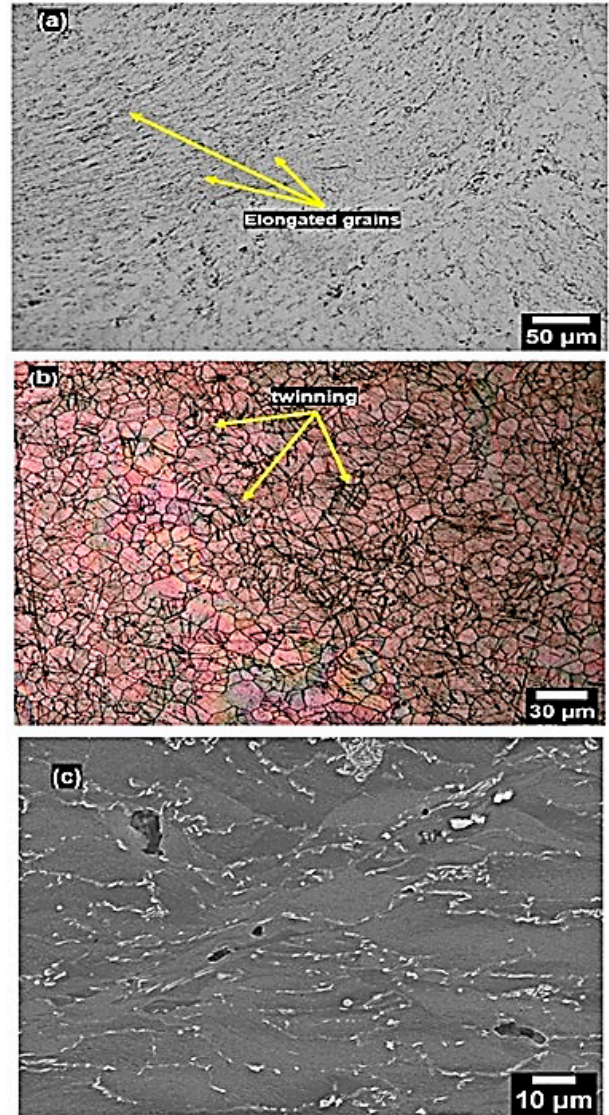


Figure 2. Rolled samples of magnesium alloy as seen by optical microscopy (a, b) and electron scanning microscopy (c).

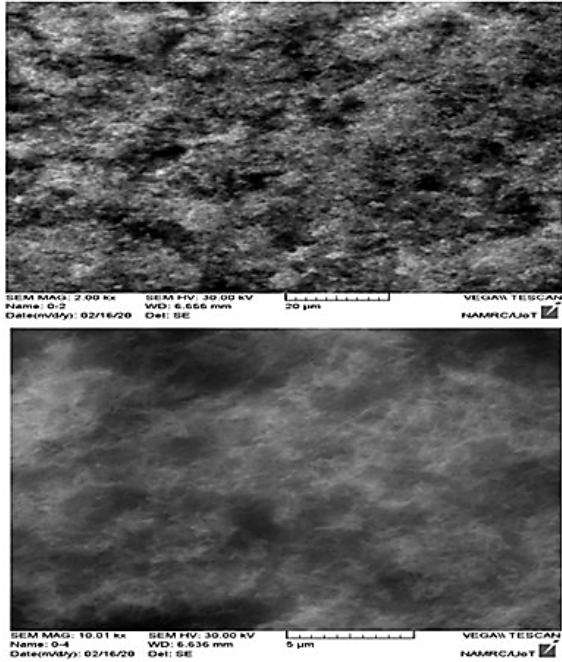


Figure 3. SEM micrograph for Mg-Al Rolled alloy and Zn-coated surface at 20 minutes with different magnifications.

A longer sputtering period can increase the average coating thickness. After 20 minutes of Zn sputtering, a coating thickness of approximately 23 μm was obtained (Figure 4) due to the higher amount of coating material deposited.

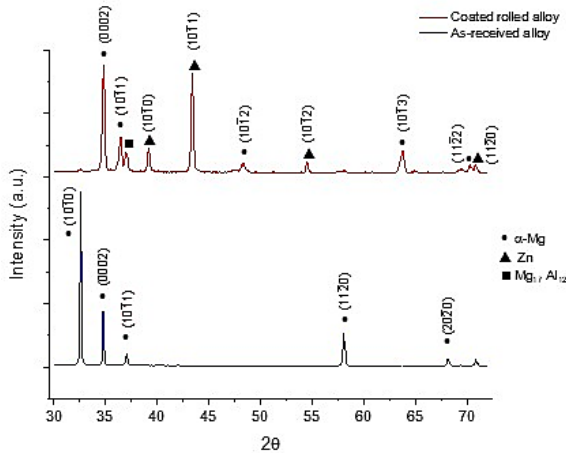


Figure 4. XRD patterns for the as-received and coated rolled sample of magnesium alloy.

Twinning has been significantly activated in the rolled alloy, as indicated by x-ray diffraction patterns, as shown in Fig. 4, compared with the as-received alloy. Slip and Twinning are the standard mechanisms of deformation

at room temperature in HCP metals such as magnesium and titanium. The activation of additional twinning was found to accompany the imposed deformation under rolling conditions and to improve the limited ductility of the magnesium alloy. The unidirectional nature of the rolling process has reoriented the deformed grains towards the rolling direction, resulting in the domination of slip during deformation. However, the presence of slip was not sufficient under these deformation conditions, which called for twinning to accommodate slip at higher rolling passes (Abud et al., 2021; El-Hafeez et al., 2023)

The rolling processing of the current magnesium alloy was conducted at room temperature, except for higher-reduction passes, which were performed at 100 °C to avoid cracking in the rolled samples. Thus, a considerable amount of strain hardening was imposed within the rolled which has led to an increase in the strength of rolled alloy compared to the as-received alloy as the deformation proceeded as shown in Fig. 5. In this figure, the strength in terms of hardness has shown an improvement as the deformation increased that expressed in terms of reduction in the thickness of rolled samples. The improvement in the strength has been raised from the accumulation of high density of dislocations during grain subdivisions and refinement, as well as the activation of different deformation mechanisms such as basal slip, twinning, and non-basal slip. All these activities have collectively increased the strain hardening in the rolled samples compared to the as-received samples and thus increased the resultant strength. Moreover (Jebur et al., 2022), the existence of β-Mg<sub>17</sub>Al<sub>12</sub> fine particles may introduce a contribution to the strengthening by hindering the moving dislocations.

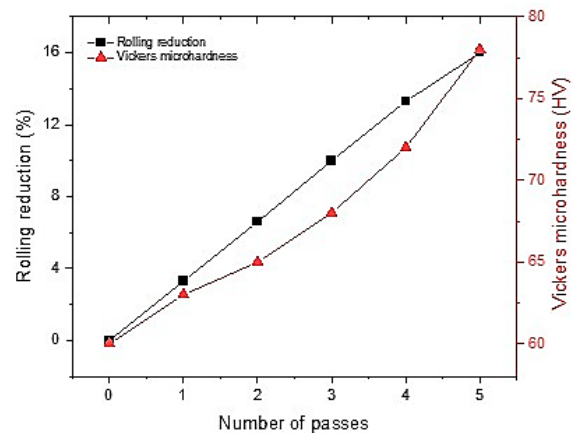


Figure 5. Variation of rolling reduction and microhardness with the number of rolling passes.

#### 4. Geometric Optimization

In this section, the magnesium-aluminum alloy and Zn Nano-coated alloy are designed and the geometric optimization calculations are performed using Gaussian 06 View software and Gaussian 09 software package, by time-dependent density functional theory (TDDFT) with B3LYP function (Lu et al., 2019; Friedlmeier et al., 1999) and basis set 6-31G (d,p), respectively (Hao et al., 2019; Hasan et al., 2022; AL-Abass et al., 2023; Hayat, 2022).

Figure 6 shows the structural geometric designs of the alloy before and after adding Zn Nano-coating, while Figure 7 shows the electronic transitions of the composites under study.

The results showed the physical-chemical compatibility of the elements and their good geometric arrangement during crystallization and coordination, as evidenced by XRD and SEM. We also note the presence of a convergence between the HOMO (Highest Occupied Molecular Orbital) and LUMO (Lowest Unoccupied Molecular Orbital) levels of the two models, which indicates a decrease in the energy gap ( $E_g$ ) values, which indicates an increase in their ability to enhance the properties of Mg-Al alloys for applications in transportation industries (Lu et al., 2019; Ali et al., 2024; Hassan et al., 2024b), as shown in Table (2).

Also, through the electronic simulation calculations, we notice an increase in the chemical hardness ( $\eta$ ) of the Mg-Al alloy and the Zn Nano-coating alloy, while maintaining good chemical softness (S) values. This is in addition to the increase in hardness with deformation, indicated by the decrease in the thickness of the rolled sample, as shown in Table 2. In addition, this combination of mechanical hardening and nano-coating improved the mechanical properties and corrosion resistance of Mg alloys (Li et al., 2014; Liu et al., 2022; Hasan et al., 2024c).

Also, while we notice a decrease in the values of chemical potential ( $\mu$ ) for the samples under study, which have a great relationship with corrosion resistance, because when a metal is exposed to corrosion, a chemical reaction occurs between the metal and the surrounding environment, leading to a change in its physical and chemical properties (Daniel et al., 2023), as shown in Table (2).

Therefore, the ( $\mu$ ) can stimulate the corrosion process, as it can lead to stimulating electrochemical reactions that increase the rate of corrosion. Accordingly, when choosing a corrosion-resistant coating or a metal protection technology, the ( $\mu$ ) that the metal will be exposed to must be taken into account.

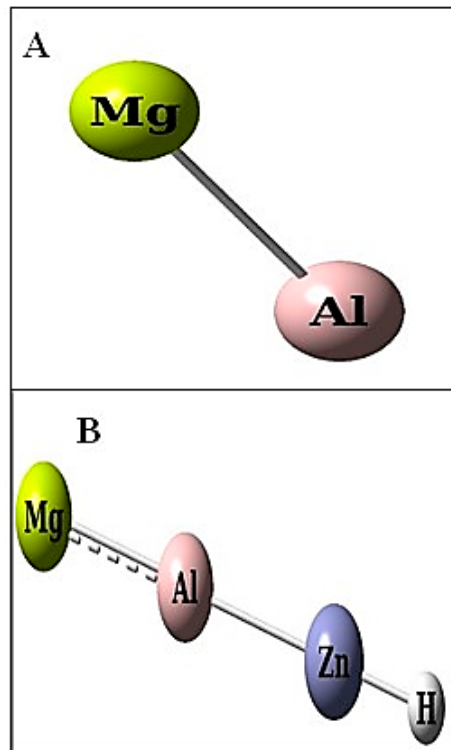


Figure 6. Structure of (A) Mg-Al alloy and (B) adding Zn Nano-coating.

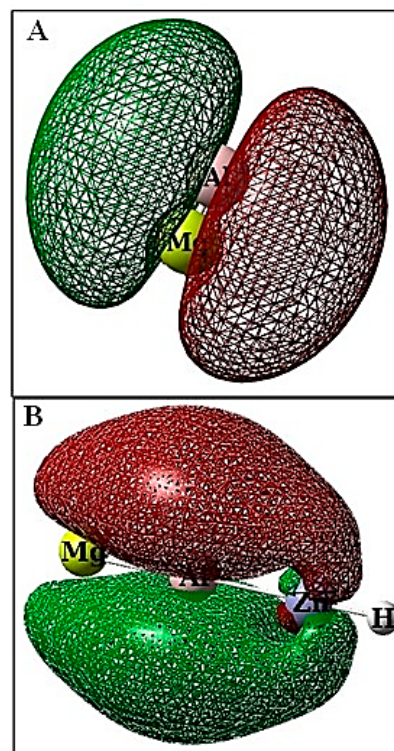


Figure 7. The shapes of HOMO and LUMO for (A) Mg-Al alloy and (B) adding Zn Nano-coating.

Table 2. Calculation of HOMO energies (EHOMO), LUMO energies (ELUMO), electronic band gap (E<sub>g</sub>), chemical potential (μ), chemical hardness (η), and chemical softness (S) via using TDDFT B3LYP/6-31 (d,p) calculation in (eV).

Sample	HOMO	LUMO	E <sub>g</sub>	μ
Mg-Al alloy	-12.1240	-8.3254	3.799	10.225
adding Zn Nano-coating	-14.2410	-8.9865	5.255	11.614

## Conclusions

An Mg-8.5%Al alloy was targeted for two modification procedures to improve bulk mechanical properties and surface corrosion resistance. This was achieved by using cold and warm rolling (Hardening) and by nanocoating a thin zinc surface layer via sputtering. This combination of mechanical hardening and Nano-coating succeeded in improving the mechanical properties and corrosion resistance of Mg alloys throughout:

- The rolled alloy showed a deformed microstructure and was refined with the fragmentation in the β-phase. The average grain size was about 10 μm, and the particle size of the β-phase was about 1 μm.
- Twinning has been activated in the rolled alloy significantly, as indicated by the X-ray diffraction patterns in comparison with the as-received alloy.
- The strength in terms of hardness has shown an improvement due to the accumulation of a high density of dislocations during grain subdivisions and refinement.
- Accordingly, a Zn Nano-coating was chosen, whose layers help mitigate the harmful effects of chemical stresses on the metal, thereby improving its corrosion resistance. Thus, processes such as plating or Zn Nano-coating provide chemical protection by forming an insulating layer that prevents direct contact between the metal and the external environment. The aim of this study was to improve the mechanical properties and corrosion resistance of magnesium-aluminum alloys, which are known for their reactivity and susceptibility to degradation.
- A decrease in the values of chemical potential (μ) for the samples was noticed by geometric optimization, which has a great relationship with corrosion resistance.

## Conflict of interest

The authors have no conflict of interest to declare.

## Funding

The authors received no specific funding for this work.

## References

- A Akraa, M., Hasan, A. S., & Kadhim, M. J. H. (2020). Spectroscopy characterization of ethylene vinyl acetate degradation by different kinds of accelerated aging. *Baghdad Science Journal*, 17(3), 20.  
<https://doi.org/10.21123/bsj.2020.17.3.0795>
- Abud, S. H., Hasan, A. S., Almaamori, M., & Bayan, N. (2021, March). Enhancement the ability to pump crude oil using rubber solutions. In *Journal of Physics: Conference Series* (Vol. 1818, No. 1, p. 012235). IOP Publishing.  
<https://doi.org/10.1088/1742-6596/1818/1/012235>
- Al-Abass, S. F. A., Braihi, A. J., & Hasan, A. S. (2023, September). Oil spill cleaning up by polymeric sorbents using salt leaching method. In *AIP Conference Proceedings* (Vol. 2839, No. 1, p. 020024). AIP Publishing LLC.  
<https://doi.org/10.1063/5.0171315>
- Al-Maamori, M. H., Al-Jamal, A. N., Habeeb, S. A., Hassan, A. S., & Majdi, H. S. (2024). Al<sup>3+</sup>-modified ZnO thin film sensor fabricated by the sputtering method: Characterization and a carbon monoxide gas detection study. *Journal of Chemical Research*, 48(1), 17475198231221453.  
<https://doi.org/10.1177/17475198231221453>
- Ali, Z. H., Hasan, A. S., & Braihi, A. J. (2024, February). Synthesis, Characterization, and Infrared Blocking Efficiency of Polyvinyl Alcohol Composites Filled with Cadmium Sulfide and Zinc Sulfide NPs. In *Annales de Chimie Science des Matériaux* (Vol. 48, No. 1).  
<https://doi.org/10.18280/acsm.480109>
- Ang, H. Q. (2021). Anelastic behaviour of commercial die-cast magnesium alloys: effect of temperature and alloy composition. *Materials*, 14(23), 7220.  
<https://doi.org/10.3390/ma14237220>

- Ata, M. H., Abdel-Gaber, G. T., Elkady, O., Fathy, M., & Abu-Okail, M. (2022). An Investigation on microstructural and mechanical properties of an innovative hybrid AA1050/Ni-Cu-Fe via mechanical alloying and friction stir processing. *CIRP Journal of Manufacturing Science and Technology*, 39, 372-386.  
<https://doi.org/10.1016/j.cirpj.2022.10.001>
- Daniel, S., Banerjee, N., Majumder, M., & Vishweshwara, S. C. (2023). Effect of Mg on Al-Mg Alloy and Electroless Ni-P Codeposition of nano-Al<sub>2</sub>O<sub>3</sub>: Mechanical, Wear, and Corrosion Resistance Properties. *Trends in Sciences*, 20(10), 6793-6793.  
<https://doi.org/10.48048/tis.2023.6793>
- El-Hafeez, G. M. A., El-Rabeie, M. M., El-Alem, Y. A., Moustapha, M. E., Fekry, A. M., & Farag, Z. R. (2023). Electrochemical Corrosion and Hydrogen Evolution Behavior for Mg and Mg-Al Alloys in Sea Water. *Journal of Bio-and Tribo-Corrosion*, 9(2), 25.  
<https://doi.org/10.1007/s40735-023-00744-x>
- Friedlmeier, G., Arakawa, M., Hirai, T., & Akiba, E. (1999). Preparation and structural, thermal and hydriding characteristics of melt-spun Mg-Ni alloys. *Journal of Alloys and Compounds*, 292(1-2), 107-117.  
[https://doi.org/10.1016/S0925-8388\(99\)00285-6](https://doi.org/10.1016/S0925-8388(99)00285-6)
- Göken, J., Bohlen, J., Hort, N., Letzig, D., & Kainer, K. U. (2003). New development in magnesium technology for light weight structures in transportation industries. In *Materials Science Forum* (Vol. 426, pp. 153-160). Trans Tech Publications Ltd.
- Hao, X., Nie, H., Ye, Z., Luo, Y., Zheng, L., & Liang, W. (2019). Mechanical properties of a novel fiber metal laminate based on a carbon fiber reinforced Zn-Al alloy composite. *Materials Science and Engineering: A*, 740, 218-225.  
<https://doi.org/10.1016/j.msea.2018.10.050>
- Hassan, H. B., Hasan, A. S., & Hashim, A. (2024a). Synthesis and boosting the structural, optical and electronic characteristics of PS/SiC/In<sub>2</sub>O<sub>3</sub> promising nanohybrid structures for tailored optoelectronics applications. *Optical and Quantum Electronics*, 56(2), 272.  
<https://doi.org/10.1007/s11082-023-05904-4>
- Hassan, H. B., Hasan, A. S., & Hashim, A. (2024b). Fabrication and advanced optical and electronic characteristics of PVA/SiC/CeO<sub>2</sub> hybrid nanostructures for augmented nanoelectronics and optics fields. *Optical and Quantum Electronics*, 56(3), 309.  
<https://doi.org/10.1007/s11082-023-05940-0>
- Hasan, A. S., Hassan, H. B., & Hashim, A. (2024c). Synthesis and unraveling the optical and electronic characteristics of PVA/Co<sub>2</sub>O<sub>3</sub>/Fe<sub>2</sub>O<sub>3</sub> hybrid nanostructures for promising nanoelectronics and photonics applications. *Optical and Quantum Electronics*, 56(4), 634.  
<https://doi.org/10.1007/s11082-023-06039-2>
- Hasan, A. S., Hassan, H. B., Hashim, A., Hasan, N. B., & Al-kawaz, Y. A. (2024d). Modeling, fabrication and characteristics of novel (PVA-SiC-In<sub>2</sub>O<sub>3</sub>) nanohybrid structures for optoelectronic applications. *Silicon*, 16(9), 4125-4138.  
<https://doi.org/10.1007/s12633-024-02991-0>
- Hasan, A. S., Mohammed, F. Q., & Takz, M. M. (2020). Design and synthesis of graphene oxide-based glass substrate and its antimicrobial activity against MDR Bacterial Pathogens. *J. Mech. Eng. Res. Dev*, 43(1), 11-17.
- Hasan, A. S., Mousa, A. H., & Hussein, A. R. A. (2022). Molecular Dynamics Simulation of SWCNT/PYA in sensors application. In *2022 Muthanna International Conference on Engineering Science and Technology (MICEST)* (pp. 83-88). IEEE.  
<https://doi.org/10.1109/MICEST54286.2022.9790266>
- Hayat, F. (2022). Electron beam welding of 7075 aluminum alloy: microstructure and fracture properties. *Engineering Science and Technology, an International Journal*, 34, 101093.  
<https://doi.org/10.1016/j.jestch.2022.101093>
- Jebur, S. K., Braihi, A. J., & Hassan, A. S. (2022). Graphene effects on the structural, morphological and optical properties of PEDOT: PSS thin films. *Materials Today: Proceedings*, 49, 2733-2740.  
<https://doi.org/10.1016/j.matpr.2021.09.255>
- Kadem, B. Y., Akraa, M., & Hassan, A. K. (2020). PVA: PEDOT: PSS: carbon based nano-composites for pressure sensor applications. *Dig. J. Nanomater. Biostructures*, 15(April), 197-205.
- Kadhim, M. H., Hasan, A. S., Akraa, M. A., & Layla, A. Y. (2021). Preparation and optimization of heterojunction donor (DLC)-acceptor (SI) as a solar cell by DFT and PLD. *Journal of Ovonic Research Vol*, 17(3), 273-281.  
<https://doi.org/10.15251/JOR.2021.173.273>
- Li, D. S., Ahzi, S., M'Guil, S., Wen, W., Lavender, C., & Khaleel, M. A. (2014). Modeling of deformation behavior and texture evolution in magnesium alloy using the intermediate  $\phi$ -model. *International Journal of Plasticity*, 52, 77-94.  
<https://doi.org/10.1016/j.ijplas.2013.06.005>

- Liu, Y., Wang, G., Chen, Y., Kang, Q., Luo, S., Li, Z., ... & Sui, X. (2022). Air atmosphere diffusion bonding of Al–Mg–Li alloy using Cu nano-coating interlayer: Microstructural characterization and formation mechanisms. *Materials & Design*, 215, 110431.  
<https://doi.org/10.1016/j.matdes.2022.110431>
- Lu, Y., Taheri, F., & Gharghour, M. (2011). Monotonic and Cyclic Plasticity Response of Magnesium Alloy. Part I. Experimental Response of a High-Pressure Die Cast AM60B. *Strain*, 47, e15-e24.  
<https://doi.org/10.1111/j.1475-1305.2008.00514.x>
- Lu, Y., Gharghour, M. A., & Taheri, F. (2008). Effect of texture on acoustic emission produced by slip and twinning in AZ31B magnesium alloy: Part I: experimental results.  
<https://doi.org/10.1080/10589750802002632>
- Lu, D., Huang, Y., Duan, J., & Hou, B. (2019). A zinc-rich coating fabricated on a magnesium alloy by oxide reduction. *Coatings*, 9(4), 278.  
<https://doi.org/10.3390/coatings9040278>
- Monteiro, W. A., Buso, S. J., & Silva, L. V. (2012). Application of magnesium alloys in transport. *New features on magnesium alloys*, 1-14.  
<https://doi.org/10.5772/48273>
- Mohammed, F. Q., Edan, M. S., Hasan, A. S., & Haider, A. J. (2021). Synthesis and theoretical concepts of boron nitride nanowires grown on nitrides stainless steel surface by hybrid gas phase process. In *Key Engineering Materials* (Vol. 886, pp. 97-107). Trans Tech Publications Ltd.  
<https://doi.org/10.4028/www.scientific.net/KEM.886.97>
- Musfirah, A. H., & Jaharah, A. G. (2012). Magnesium and aluminum alloys in automotive industry. *Journal of Applied Sciences Research*, 8(9), 4865-4875.
- Nikulin, I., Kipelova, A., Gazizov, M., Teleshov, V., Zakharov, V., & Kaibyshev, R. (2010). Novel Al-Cu-Mg-Ag alloy for high temperature applications. *12th ICAA, Japan*, 2303-2308.
- Sharma, S., Patyal, V., Sudhakara, P., Singh, J., Petru, M., & Ilyas, R. A. (2021). Mechanical, morphological, and fracture-deformation behavior of MWCNTs-reinforced (Al–Cu–Mg–T351) alloy cast nanocomposites fabricated by optimized mechanical milling and powder metallurgy techniques. *Nanotechnology Reviews*, 11(1), 65-85.  
<https://doi.org/10.1515/ntrev-2022-0005>
- Wang, R. M., Eliezer, A., & Gutman, E. M. (2003). An investigation on the microstructure of an AM50 magnesium alloy. *Materials Science and Engineering: A*, 355(1-2), 201-207.  
[https://doi.org/10.1016/S0921-5093\(03\)00065-0](https://doi.org/10.1016/S0921-5093(03)00065-0)